

## SEISMIC RESISTANCE OF HIGH STRENGTH CONCRETE COLUMNS

D. GALEOTA and M.M. GIAMMATTEO

Department of Structural Engineering of L'Aquila, University of L'Aquila  
L'Aquila, ITALY

R. MARINO

Calcestruzzi S.p.A.  
Ravenna, ITALY

### ABSTRACT

The aim of this study was to examine the structural behavior, under loads simulating earthquake effects, of concrete columns designed with different amounts of longitudinal and transverse reinforcement. The columns were constructed with concrete having compressive strength in the range of 80 MPa. On the basis of experimental results, analytical models and design procedures for earthquake resistant columns were tested.

### KEYWORDS

High strength concrete columns; axial load; cyclic flexure; analytical model; confinement index; plastic hinge length; design procedure.

### INTRODUCTION

There is still limited knowledge of the behavior of high strength concrete structural elements, when subjected to severe earthquakes. In particular, very few experimental studies of great interest are reported in the technical literature on strength and deformability of columns constructed with high strength concrete (Azizinamini *et al.*, 1994; Park, 1994; Shah and Ahmad, 1994; Sheikh *et al.*, 1994; Thomsen *et al.*, 1994).

A research program has been undertaken at the University of L'Aquila to develop design information for earthquake resistant high strength concrete structural elements. The current phase of this program has been that of providing experimental results of recent tests on reinforced concrete columns subjected to axial load and cyclic flexure. The variables examined were the amount of longitudinal and transverse reinforcement and the level of axial load. The experimental results provided useful data to test and to calibrate analytical models and design procedures for earthquake resistant high strength concrete columns.

### TEST PROGRAM

Twenty-four large-scale columns were constructed and tested under simulated earthquake load conditions. The overall dimensions of the units and the details of the reinforcement are shown in Fig. 1. The experimental variables used in testing were the amount of the transverse and longitudinal reinforcement and the level of column axial load. The applied levels of compressive axial load were  $0.2f_{c0}A_c$  and  $0.3f_{c0}A_c$ , where  $f_{c0}$  is the

compressive cylinder strength (80 MPa) and  $A_c$  the gross cross-sectional area of the column. The concrete mix was prepared in order to obtain an average specific compressive cylinder strength at 28 days of age ( $f_{c0} \cong 80$  MPa). Deformed reinforcing bars (Feb44k,  $f_{yk} \geq 430$  MPa) were used for longitudinal and transverse reinforcement. After applying a constant axial load (N) to the column (1 MN or 1.5 MN), the stub (fig. 1) was cyclically loaded by a double-acting actuator. During testing, important parameters such as loads, displacements, column curvatures, strains in the longitudinal and transverse reinforcement were continuously recorded for each column (Galeota *et al.*, 1996).

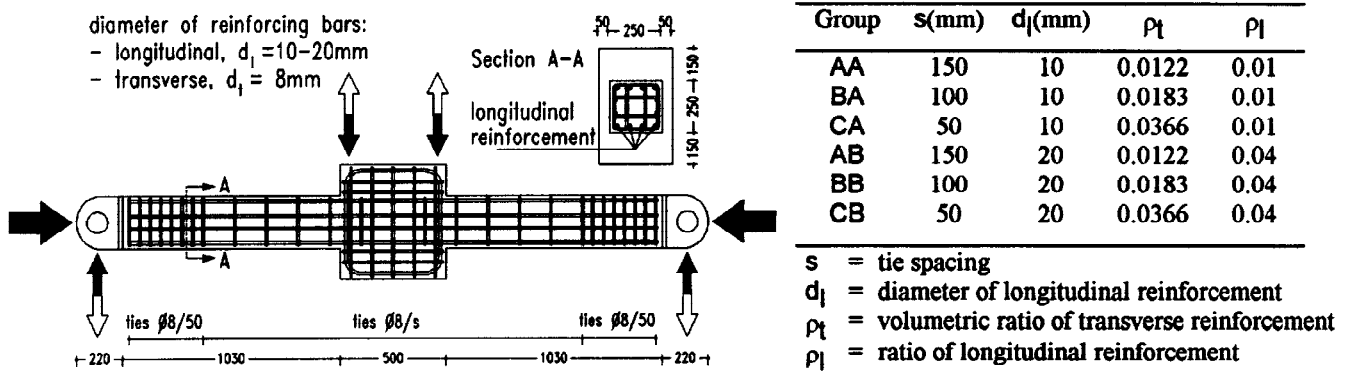


Fig. 1. Dimensions and details of column test units.

## PREDICTIONS OF ULTIMATE BEHAVIOR OF COLUMNS

A computer program was written to compute the monotonic moment-curvature relationships for uniaxially eccentrically loaded columns. The program was based on the model proposed by Cusson and Paultre (1995) for confined and unconfined high strength concrete in compression, as described in Fig. 2. The descending part of the stress-strain curve for confined concrete was followed until the stress dropped to 35% of the compressive strength, beyond this point a horizontal line was assumed to represent the concrete behavior.

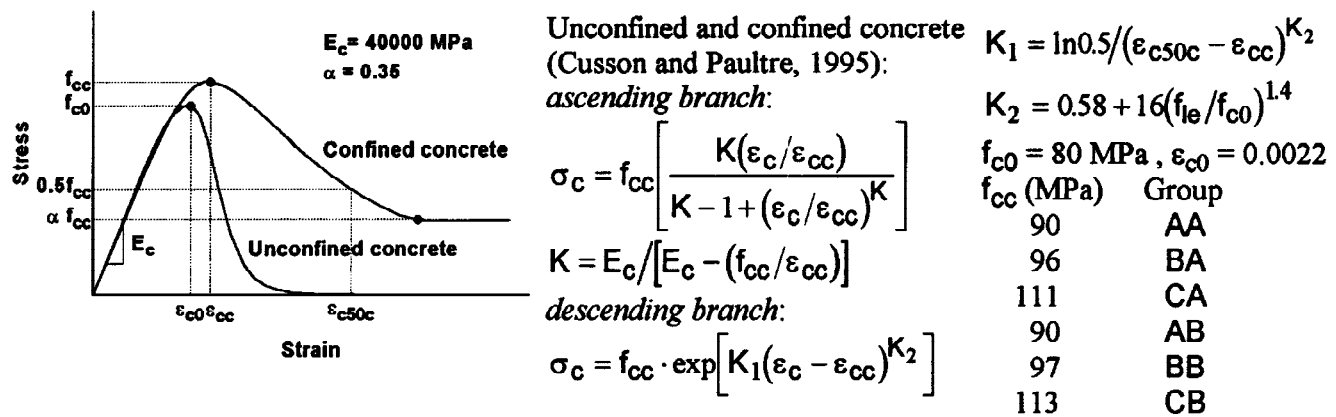


Fig. 2. Analytical stress-strain curves of confined and unconfined concrete.

A new indicator of confinement efficiency was proposed by Cusson and Paultre (1995) as:

$$\text{Effective confinement index} = f_{le} / f_{c0}$$

where:  $f_{le}$  = the effective confinement pressure applied to the concrete core;  
 $f_{c0}$  = the compressive strength of the unconfined concrete.

According to the effective confinement index, the test units were classified into two classes: medium confinement (groups CA and CB with  $f_{le}/f_{c0} \cong 9\%+10\%$ ) and low confinement (groups AA, BA, AB, and BB with  $f_{le}/f_{c0} \cong 1.7\%+3.8\%$ ).

When the test units reached their maximum strength, the strains  $\epsilon_{hc}$  in the transverse reinforcement and the strains  $\epsilon_{cc}$  in the extreme fibres of the concrete core were calculated following the procedure suggested by Cusson and Paultre (1995).

Table 1 shows the comparison between the measured and calculated strain values in some test units. In general, the test units with low confinement showed strains in the transverse reinforcement lower than the yield strain.

Table 1. Comparison of experimental and calculated strain values.

Unit (N = 1 MN)	$\epsilon_{hc}$		$\epsilon_{cc}$	
	Experimental	Calculated	Experimental	Calculated
AA3	1.7e-04	0.0012	0.0021	0.0025
BA4	3.6e-04	0.0015	0.0015	0.0030
CA1	5.3e-04	0.0027	0.0024	0.0059
AB1	5.8e-04	0.0013	0.0020	0.0026
BB1	0.0026	0.0016	0.0024	0.0032
CB1	0.0050	0.0030	0.0060	0.0065

The stress-strain curves of the longitudinal reinforcing steel were analytically expressed as shown in Fig. 3. A, B, C and D are four constants determined from the boundary conditions (Wang, Shah and Naaman, 1987). Both the experimental and analytical curves are shown in Fig. 3.

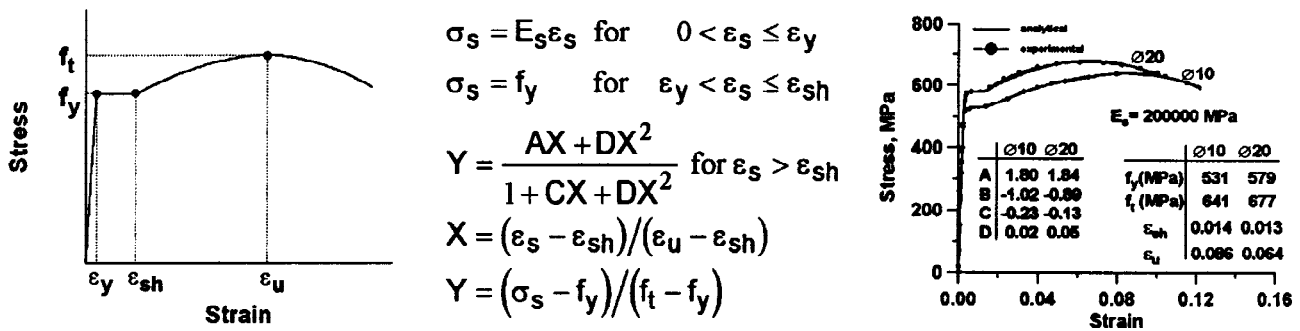


Fig. 3. Analytical and experimental stress-strain curves of longitudinal reinforcement.

The moment-curvature relationships for all groups of test units were computed and the experimental and analytical maximum moment capacities for each unit are shown along with their ratios in Table 2. The ratios of experimental to analytical moment capacities ranged from 0.92 to 1.37. It can be seen that a satisfactory conservative comparison was obtained.

The predicted moment-curvature relationships were compared with the experimental relationships (Fig. 4). It can be seen that the predicted monotonic moment-curvature relationships can be regarded as an envelope for the experimental cyclic behavior of the columns.

Table 2. Experimental and theoretical moment capacities.

Unit	Axial load (MN)	Experimental moment (kNm)	Analytical moment (kNm)	$M_{exp}/M_{an.}$
AA3	1.0	126.978	129.085	0.984
AA4	1.0	169.747	129.085	1.315
AA1	1.5	167.518	153.991	1.088
AA2	1.5	162.883	153.991	1.058
BA1	1.0	176.388	129.016	1.367
BA4	1.0	140.710	129.016	1.091
BA2	1.5	167.365	154.243	1.085
BA3	1.5	172.041	154.243	1.115
CA1	1.0	132.275	127.665	1.036
CA3	1.0	164.674	127.665	1.290
CA2	1.5	172.102	150.195	1.149
CA4	1.5	174.852	150.195	1.164
AB1	1.0	214.887	223.717	0.961
AB4	1.0	254.164	223.717	1.136
AB2	1.5	224.557	244.344	0.919
AB3	1.5	230.044	244.344	0.941
BB1	1.0	210.096	223.440	0.940
BB2	1.0	236.700	223.440	1.059
BB4	1.5	240.897	247.039	0.975
BB4	1.5	246.715	247.039	0.999
CB1	1.0	224.465	233.926	0.960
CB2	1.0	222.658	233.926	0.952
CB3	1.5	244.387	253.931	0.962
CB4	1.5	251.144	253.931	0.989

The load-top displacement envelopes of the columns were calculated by integrating the moment-curvature relationship and by considering the slippage of longitudinal reinforcement at the column-stub interface. Load-top displacement comparison of selected test units are shown in Fig. 5.

The measurement of column curvature  $\Phi$  allowed the calculation of the equivalent plastic hinge length  $L_p$  from the following equation:

$$\Delta = \Delta_y + (\Phi - \Phi_y)L_p(L - 0.5L_p) \quad (1)$$

where:  $\Delta$  = current displacement,  
 $\Delta_y$  = yield displacement,  
 $\Phi_y$  = yield curvature,  
 $L$  = length of column.

Equation (1) can be written as

$$L_p = L - \sqrt{L^2 - 2(\delta_d - 1)\frac{\Delta_y}{\Phi - \Phi_y}} \quad (2)$$

where:  $\delta_d = \Delta/\Delta_y$  (displacement ductility factor).

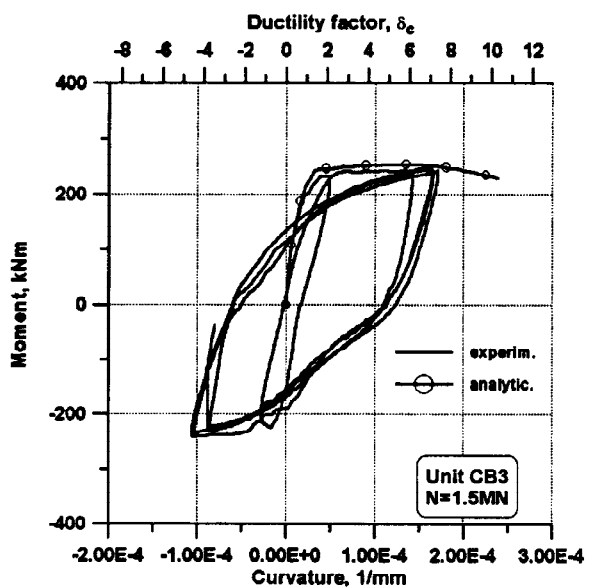
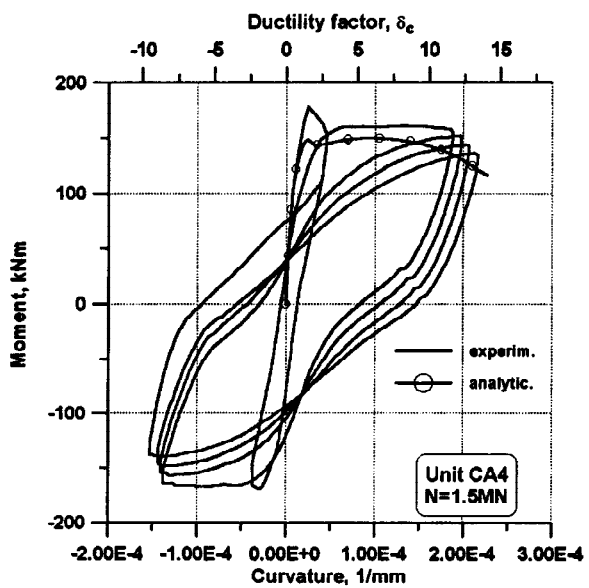
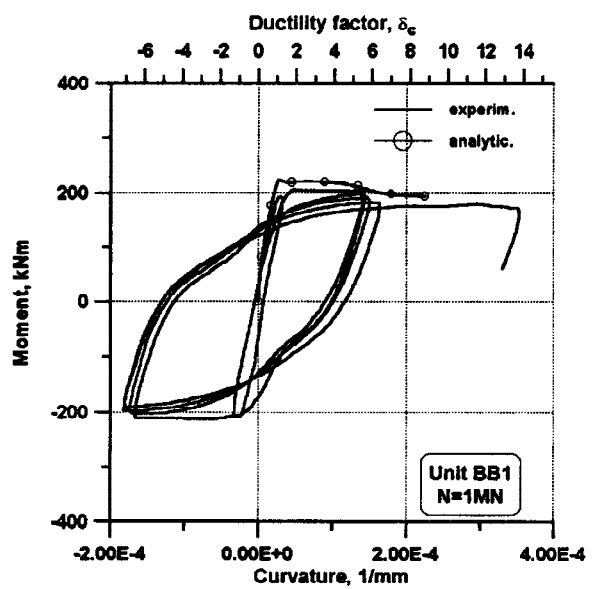
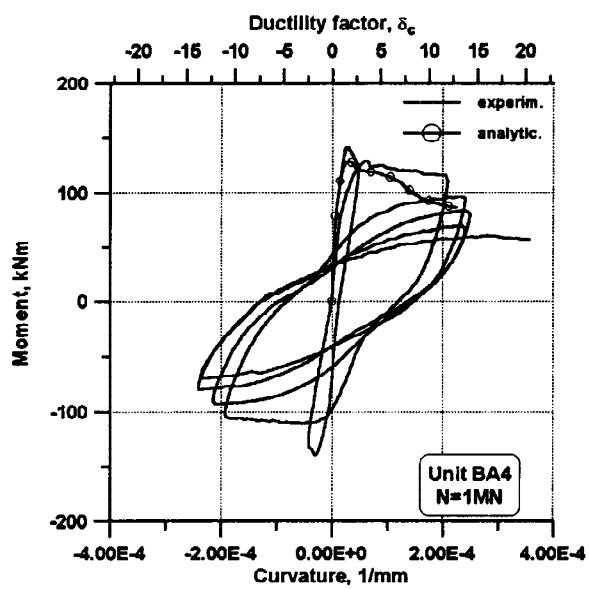
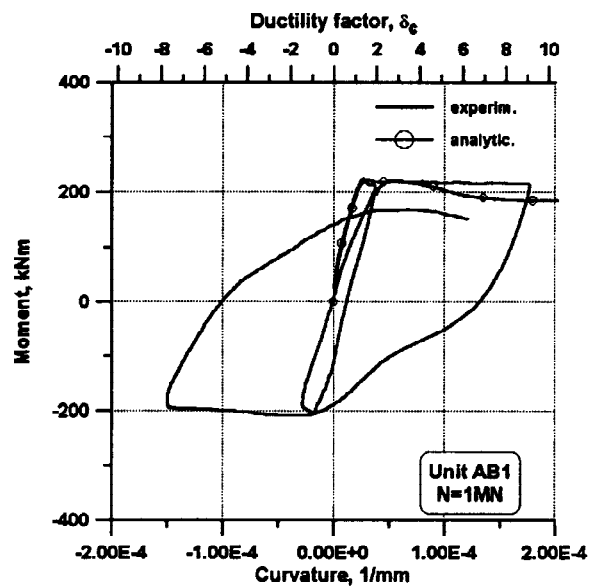
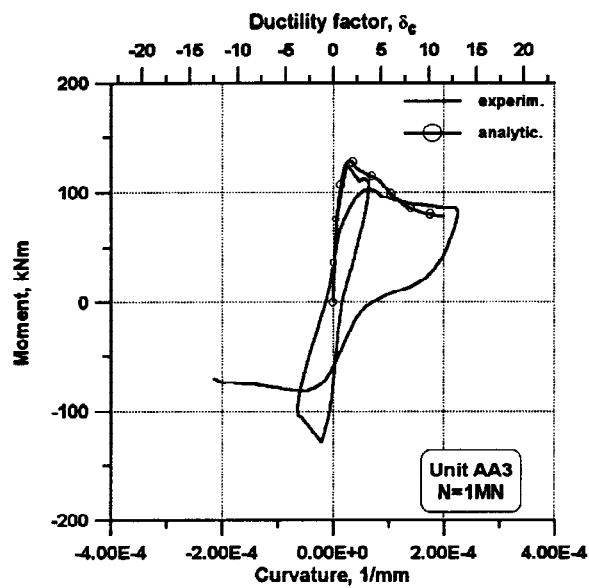


Fig. 4. Predicted and experimental moment-curvature relationships.

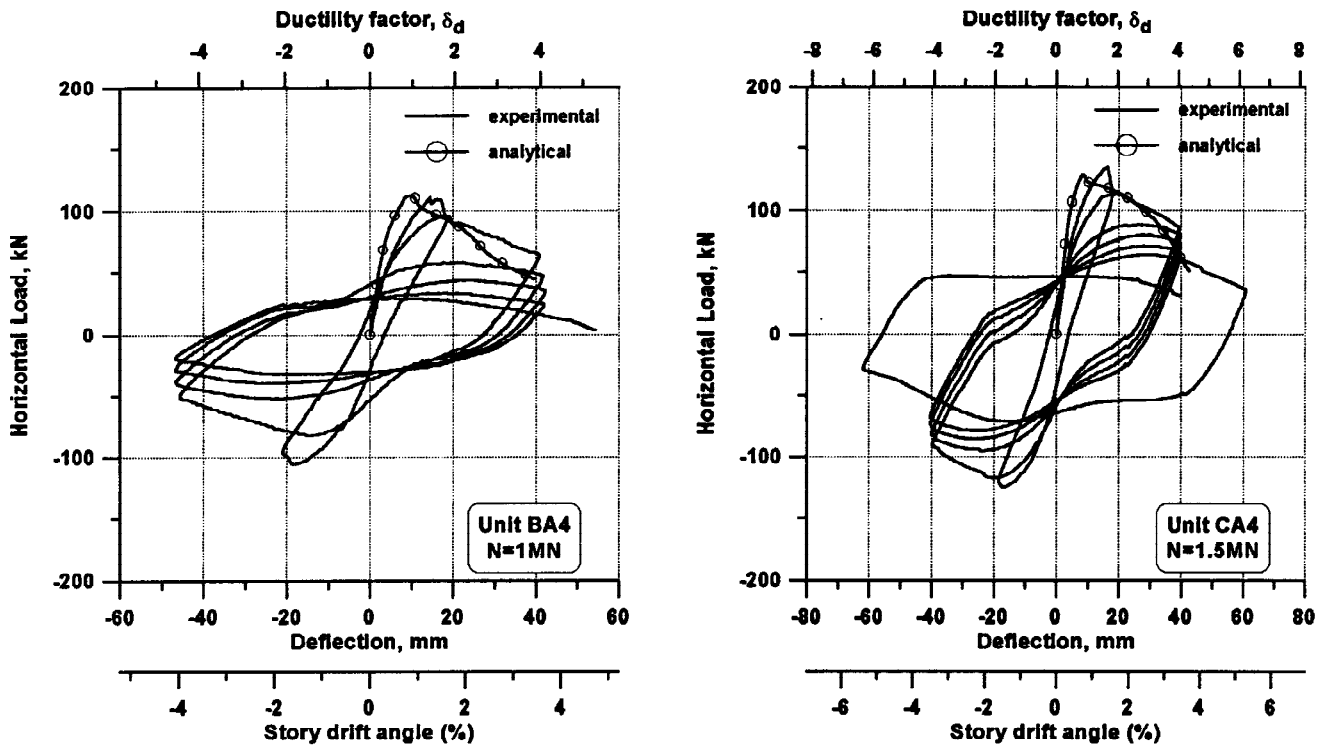


Fig. 5. Predicted and experimental load-top displacement.

Figure 6 shows the ratio  $L_p/h$  versus the displacement ductility factor, where  $h$  is the section size of the column (250 mm). It appears that the equivalent plastic hinge lengths ranged from  $0.4h$  to  $1.1h$  and resulted slightly dependent on the amount of longitudinal reinforcement.

The load-moment interaction curves (Fig. 7) were calculated according to the assumptions of the CEB Bulletin n.228 (1995), by using the actual strengths for longitudinal reinforcing steel and concrete ( $\gamma_s = 1$ ,  $\gamma_c = 1$ ). The load-moment interaction curves were compared to the experimental peak strength of the units. It can be seen that the results predicted by the CEB method are conservative and close to the experimental data.

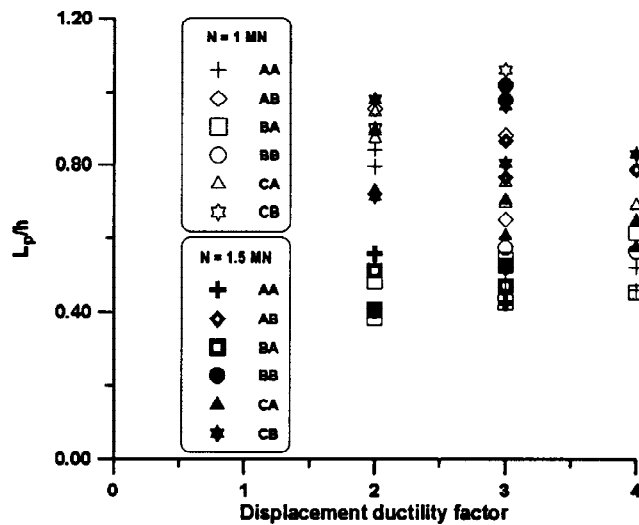


Fig. 6.  $L_p/h$  ratio versus displacement ductility factor.

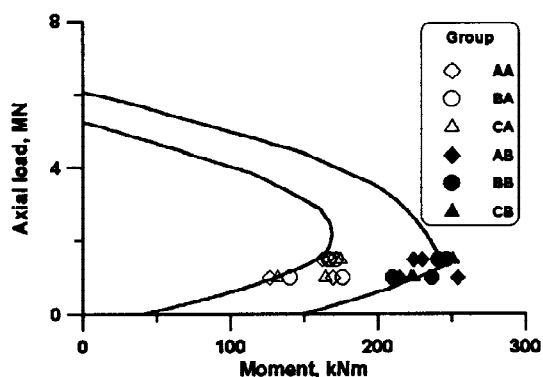


Fig. 7. Load-moment interaction curves according to CEB Bull. n.228, compared with the experimental peak strength of the units.

## CONCLUSIONS

1. The model of Cusson and Paultre to predict the stress-strain curve of high strength concrete (confined and unconfined) was used to compute the monotonic moment-curvature relationships for uniaxially eccentrically loaded columns. The predicted ultimate loads, moments, curvatures and displacements satisfactorily corresponded to the experimental results of testing.
2. On the basis of the measured column curvatures, the equivalent plastic hinge length was calculated for each test unit, for the load cycles corresponding to a displacement ductility factor equal to 2, 3 and 4. The equivalent plastic hinge length ranged from 0.4 to 1.1 times the section size of the column.
3. The load-moment interaction curves calculated according to the assumptions of the CEB Bulletin d'Information n.228, satisfactorily predicted the experimental peak strength values of the test units.

## ACKNOWLEDGEMENT

This study was supported by the financial assistance of the Ministry of University and Scientific Research (MURST 40%), Italy.

## REFERENCES

- Azizinamini, A., S.S.B. Kuska, P. Brungardt and E. Hatfield (1994). Seismic behavior of square high strength concrete columns. *ACI Structural Journal*, **91** no. 3, 336-345.
- CEB Bulletin d'Information n.228 (1995). *High performance concrete - Recommended extensions to the Model Code 90*. Report of the CEB-FIP Working Group on High strength/High performance concrete.
- Cusson, D. and P. Paultre (1995). Stress-strain model for confined high strength concrete. *ASCE Journal of Structural Engineering*, **121** no.3, 468-477.
- Galeota, D., M.M. Giammatteo and R. Marino (1996). High strength RC columns subjected to axial load and cyclic flexure. *Proc. 4th Int. Symp. on Utilization of High strength/High performance concrete*, Paris.
- High performance concretes and applications, edited by S.P. Shah & S.H. Ahmad (1994).
- Park, R. (1994). Recent seismic load tests on reinforced concrete structural elements and subassemblages at the University of Canterbury. *Proc. 10th European Conf. on Earthquake Engineering*, **3**, 2351-2360.

- Sheikh, S.A., D.V. Shah and S.S. Khoury (1994). Confinement of high-strength concrete columns. *ACI Structural Journal*, **91 no.1**, 100-111.
- Thomsen, J.H.IV and J.W. Wallace (1994). Lateral load behavior of reinforced concrete columns constructed using high-strength materials. *ACI Structural Journal*, **91 no.5**, 605-615.
- Wang, P.T., S.P. Shah and A.E. Naaman (1987). High strength concrete in ultimate strength design. *Proceedings, ASCE*, **104 ST11**, 1761-1773.